Macromolecules
ARTICLE

Macromolecules **2010**, *43*, 10457–10465

DOI: 10.1021/ma1023632

Multistimuli Responsive Polymer Nanoparticles On the basis of the Amphiphilic Azobenzene-Contained Hyperbranched Poly(ether amine) (hPEA-AZO)

Bing Yu, Xuesong Jiang,* Rui Wang, and Jie Yin*

School of Chemistry & Chemical Technology, State Key Laboratory for Metal Matrix Composite Materials, Shanghai Jiao Tong University, Shanghai, China

Received October 16, 2010; Revised Manuscript Received November 20, 2010

ABSTRACT: We here reported the multistimuli responsive behavior of polymer nanoparticles, which was formed through direct dispersion of the amphiphilic azobenzene-contained hyperbranched poly(ether amine) (hPEA-AZO) in water. A series of hPEA-AZO were synthesized by introduction of azobenzene moieties into the periphery of hyperbranched poly(ether amine) (hPEA), which was developed by our group recently. The obtained polymer nanoparticles of hPEA-AZO which were revealed by dynamic light scattering (DLS) and transmission electron microscopy (TEM), exhibited the sharp stimuli-response to temperature, pH, and ionic strength with tunable cloud point (CP) from 25 to 100 °C. CP of the obtained hPEA-AZO nanoparticles in aqueous solution decreased with the increase of azobenzene content, pH value and ionic strength, and represented a linear relationship with the azobenzene content and ionic strength. The hPEA-AZO nanoparticles also showed a light-controlled CP and size. After UV irradiation (365 nm), we observed lower value of CP and larger size for hPEA-AZO nanoparticles. The CP difference of hPEA-AZO nanoparticles in aqueous solution between before (CP_T, *trans* form) and after (CP_C, *cis* from) UV irradiation (365 nm) increased linearly upon the azobenzene content up to 5 °C

Introduction

Because of their potential applications in separation, biosensor, chemical storage and transport, and gene and drug delivery, polymer nanoparticles with response to environmental stimuli have attracted much attention.[1−6] The stimuli-responsive behaviors of polymer nanoparticles strongly depend on the external chemical and physical stimuli, such as ionic strength, light, electric and magnetic field, temperature and pH.[7−9] Because of the easy-control, light-response is becoming of special importance to polymer nanoparticles in the application fields of drug delivery[10−12] and photo sensor.[13−15] To obtain the polymer nanopaticles response to light, a variety of light-responsive moieties are introduced into the polymers which construct polymer nanoparticles. Among these light-responsive moieties, azobenzene group is most studied due to its well-known reversible isomerization from *trans*- to *cis*-configuration upon irradiation.[16−21] Several research groups reported the responsive polymer nanoparticles formed by self-assembly of amphiphilic azobenzene-contained copolymers in aqueous solution.[18,22−25] Besides response to light, some of these polymer nanoparticles exhibited the response to another stimulus such as temperature[26,27] or pH.[24] Because the behavior changes of the responsive polymer nanoparticles are often a result of their response to the combination of the environmental changes, polymer nanoparticles which are sensitive to multiple stimuli are very important in practical applications, therefore, become of very interest.[6,19,28−36] However, to the best of our knowledge, polymer nanoparticles responsive to the tetrastimuli of temperature, pH, ionic strength, and light have not yet been demonstrated.

In this text, we report polymer nanoparticles with response to the tetrastimuli of temperature, pH, ionic strength, and light, which were formed by directly self-assembly of amphiphilic azobenzene-contained hyperbranched poly(ether amine)s (hPEA-AZOs) in aqueous solution. Recently, we had developed a novel family of amphiphilic hyperbranched poly(ether amine) (hPEA), which can be obtained through one-pot synthesis.[37] These hPEAs can be directly dispersed into aqueous solution to form uniform-sized polymer nanoparticles responsive to temperature, pH and ionic strength with accurately tunable cloud point (CP). Moreover, hPEAs contain reactive amino groups in periphery, which can be further modified with functional groups easily. Motivated by the novel characteristics of hPEAs, we continued to introduce azobenzene groups into the periphery of hPEA to obtain amphiphilic azobenzene-contained hyperbranched poly(ether amine)s (hPEA-AZOs), which are expected to be directly dispersed in water to form polymer nanoparticles with response of tetra-stimuli. The responsive behavior of these resulted polymer nanoparticles was investigated in detail.

Experimental Section

Material. 4-Phenylazophenol (hydroxyl azobenzene, H-AZO) was purchased from Alfa Aesar and used without further purification. 3-Chloro-1,2-epoxypropane (ECH) was purchased from Sinopharm Chemical Reagent. Potassium carbonate (K_2CO_3) was purchased from Sinopharm Chemical Reagent and grinded into powder then dried at 110 °C for 12 h before used. Hyperbranched poly(ether amine) (hPEA211) was synthesized according to previous report.[37]

Synthesis of 4-Phenylazophenyl Glycidyl Ether (E-AZO). The reaction was conducted in a two-necked flask equipped with a nitrogen inlet and a reflux condenser. The mixture of H-AZO (0.01 mol), ECH (0.05 mol), and K_2CO_3 (0.03 mol) was refluxed in 25 mL 2-butanone for 12 h under a nitrogen atmosphere. After cooling to room temperature, the inorganic residue was filtered off and washed with 2-butanone. The filtrate solution

---

*Corresponding authors. Telephone: +86-21-54743268; Fax: +86-21-54747445. E-mail: (X.J.) ponygle@sjtu.edu.cn, (J.Y.) jyin@sjtu.edu.cn..

Scheme 1. Total Synthesis Process of hPEA-AZO

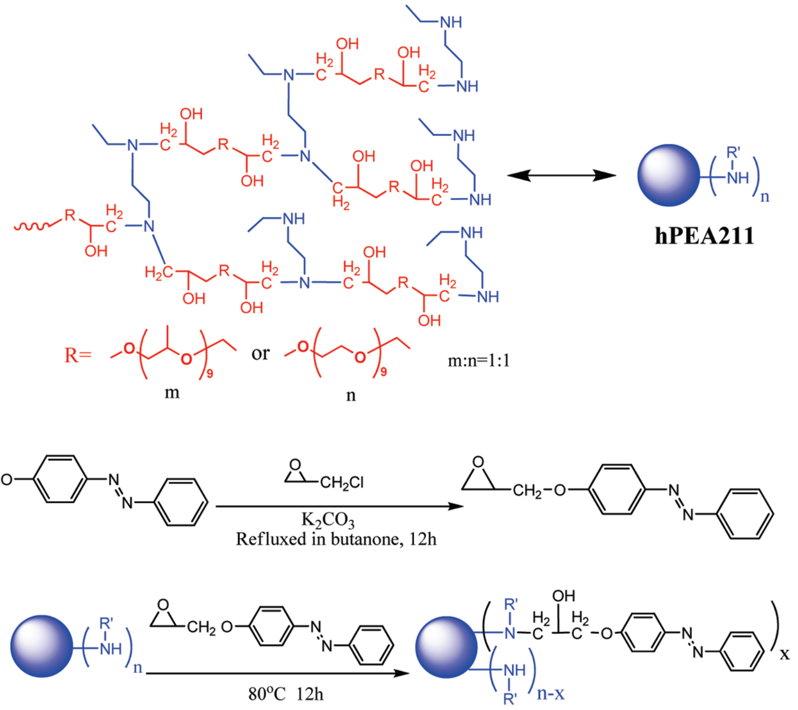

was evaporated by rotary to remove solvent and excess ECH. The crude product was purified by recrystallization in $CHCl_3$ to get E-AZO and the yield is about 97%. ^{1}H NMR (DMSO-d_6, ppm): δ 7.85, 7.53, 7.15 (aromatic, 9H), 4.45, 3.92 ($-OCH_2-$, 2H), 3.36 (CH, 1H), 2.85, 2.73 ($-CH_2-$, 2H). FT-IR (KBr): 2973 cm^{-1}, 2902 cm^{-1} (C$-$H), 1598 cm^{-1}, 1411 cm^{-1} (C$=$C in benzene), 1500 cm^{-1} (*N*$=$N), 1249 cm^{-1} (C$-$N), 1049 cm^{-1} (C$-$O).

Synthesis of hPEA211-AZOs. hPEA211-AZOs were synthesized according to Scheme 1. To the mixture of hPEA211 (0.005 mol, in terms of its structural units) and ethanol (20 mL), E-AZO was added in proportion (shown in Table 1). The reaction mixture was refluxed for 12 h with nitrogen protection. Then most of the solvent was removed by rotary evaporation and the mixture left was poured into *n*-hexane. The precipitate was washed by *n*-hexane for several times and dried in vacuum oven, and the product was named as hPEA211-AZO.

Characterization. ^{1}H NMR spectra in dimethyl sulfoxide-d_6 (DMSO-d_6) and D_2O were acquired with Varian Mercury Plus 400 MHz spectrometer equipped with a temperature control unit, respectively. The samples in DMSO-d_6 were measured at room temperature and the samples prepared as 1 wt % in D_2O were measured with the proton signal of D_2O solvent as the internal reference at 20, 40, and 60 °C, respectively.

Infrared absorption spectra (IR) measurements were carried out with Paragon 1000 Fourier transformation infrared absorption spectrometer. The samples were prepared by dropping the polymer solution onto a KBr film and dried below an infrared lamp.

The UV$-$visible spectra of the hPEA211-AZO aqueous solution were checked by a UV-2550 spectrophotometer (Shimadzu, Japan). The hPEA211-AZO aqueous solutions were prepared from 0.1 M citrate buffered aqueous solutions with 3 mg/mL copolymer concentration. These samples were exposed under an ultraviolet LED lamp (Uvata) at 365 and 450 nm with intensity about 8.4 mW/cm^2, and the UV$-$visible spectra were checked every 5 min.

The transmission electron microscopy (TEM) images were obtained using a JEM-2100 (JEOL Ltd., Japan) microscope operated at 200 kV. The sample was prepared by dropping the polymer solution onto a copper grid coated with a thin polymer film while the excess solution was removed by filter paper, and then dried at room temperature for 24 h. No staining treatment was performed for the measurement.

Table 1. Composition Data of hPEA211-AZO

polymer[a]	content of azobenzene (mole ratio) in feed[b]	content of azobenzene (mole ratio) in polymer[c]	CMC (g/L)[d]
hPEA211-AZO02	0.20	0.20	0.73
hPEA211-AZO04	0.40	0.41	0.33
hPEA211-AZO06	0.60	0.58	0.38
hPEA211-AZO08	0.80	0.79	0.36
hPEA211-AZO10	1.00	0.96	0.09

[a] hPEA211-AZO*x*, *x*/10 represent the proportion of the amino groups in hPEA211 modified by azobenzene theoretically. [b] The mole ratio in feed is calculated as the mole ratio of E-AZO and secondary amino groups in hPEA211. [c] Estimated from UV$-$visible absorption at 349 nm compared with pure 4-Phenylazophenol in THF. [d] CMC was measured by using Nile Red as a fluorescent probe.

The atom force microscopy (AFM) images were obtained by using a scanning probe microscope (Nanoscope III, Digital instruments) operated in the contacting mode. The sample was prepared by dropping dilute polymer aqueous solution on a mica sheet and then dried at room temperature for 24 h.

Cloud Point Measurements. The optical transmittance of the polymer solutions were measured at 700 nm with a spectral-1.70 UV$-$visible spectrophotometer (GBC Cintra 100, Aus.) equipped with a thermo cell at a heating rate of 1 °C/min. The temperature at 90% light transmittance of the polymer solution was defined as the cloud point (CP). The hPEA211-AZO aqueous solutions were prepared from 0.1 M citrate buffered aqueous solutions with 3 mg/mL copolymer concentration.

Critical Micelle Concentration (CMC) Measurements. The critical micelle concentration (CMC) of the hPEA211-AZO was determined by using Nile Red as a fluorescent probe.[38] Solutions of hPEA211-AZO with different concentrations were prepared by ultrapure water, and about 0.1 mg Nile Red was added into each of the samples, respectively. The solutions were sonicated for 30 min and equilibrated in the darkness overnight. The emission spectra were recorded under LS-50B luminescence

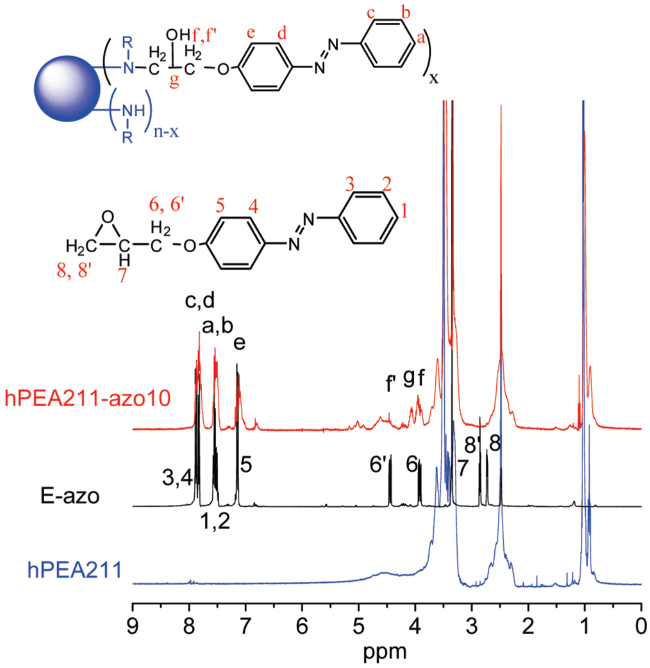

Figure 1. ^{1}H NMR spectra of hPEA211, E-AZO, and hPEA211-AZO10 in DMSO-d_6.

spectrometer (Perkin-Elmer Company, USA). The excitation wavelength was set at 550 nm, and the fluorescence emission spectra were recorded between 560 and 750 nm. All fluorescence spectra were recorded at room temperature.

Dynamic Light Scattering (DLS). The measurements were performed in the copolymer aqueous solution using a ZS90 Zetasizer Nano ZS instrument (Malvern Instruments Ltd., U.K.) equipped with a multi-τ digital time correlation and a He−Ne laser (λ = 633 nm) at an angle of 90°. The CONTIN analysis method was used. The samples were prepared in ultrapure water with 1 mg/mL copolymer concentration.

Results and Discussion

Synthesis and Characterization of hPEA211-AZOs. Our previous work showed that amphiphilic hyperbranched poly(ether amine)s (hPEAs) could be successfully synthesized through nucleophilic addition/ring-opening reaction of commercial diglycidyl ether and amine via one-pot synthesis.[37] Moreover, there were reactive amino groups in periphery of the obtained hPEAs. Because nucleophilic addition/ring-opening reaction between amine and epoxy group possesses the characteristics of "click-chemistry", hPEA can be further functionalized by molecules with epoxy groups. As a result, amphiphilic azobenzene-contained hPEAs (hPEA-AZOs) can be easily obtained by introducing azobenzene moieties into the periphery of hPEAs. The process for synthesis of hPEA-AZO is shown in Scheme 1. As azobenzene is a relative hydrophobic compound, then a relative hydrophilic hPEA (hPEA211) is chosen to ensure that the hPEA-AZO produced can be dispersed directly in water at room temperature. In the structure of hPEA211, the mole ratio of poly(propylene oxide) (PPO) chains and poly(ethylene oxide) (PEO) chains is 1:1. The successful functionalization of hPEAs with azobenzene groups was confirmed by FT-IR (Figure S1, Supporting Infomation) and ^{1}H NMR (Figure 1). Compared with hPEA211, new peak at 1580 cm^{-1} assigned to phenyl ring and new peak at 1498 cm^{-1} assigned to azo groups appeared in FT-IR spectrum of hPEA211-AZO10, indicating introduction of azobenzene to hPEA211. The structure of hPEA211-AZO10 is also supported by ^{1}H NMR spectra, and the attribution of each signal is also signed in Figure 1. In comparison with hPEA211, the existence of azobenzene groups in hPEA211-AZO10 is proved by signals of aromatic compound at ~7.15, ~7.55, and ~7.85 ppm in ^{1}H NMR spectrum of hPEA211-AZO, and a new signal appears at ~4.0 ppm, which also indicates the occurrence of the reaction between epoxy groups in E-AZO and amino groups in hPEA211. In comparison with E-AZO, the disappearance of the signals at ~2.7 and ~2.85 ppm in ^{1}H NMR spectrum of hPEA211-AZO10 proves that all the E-AZO are reacted,

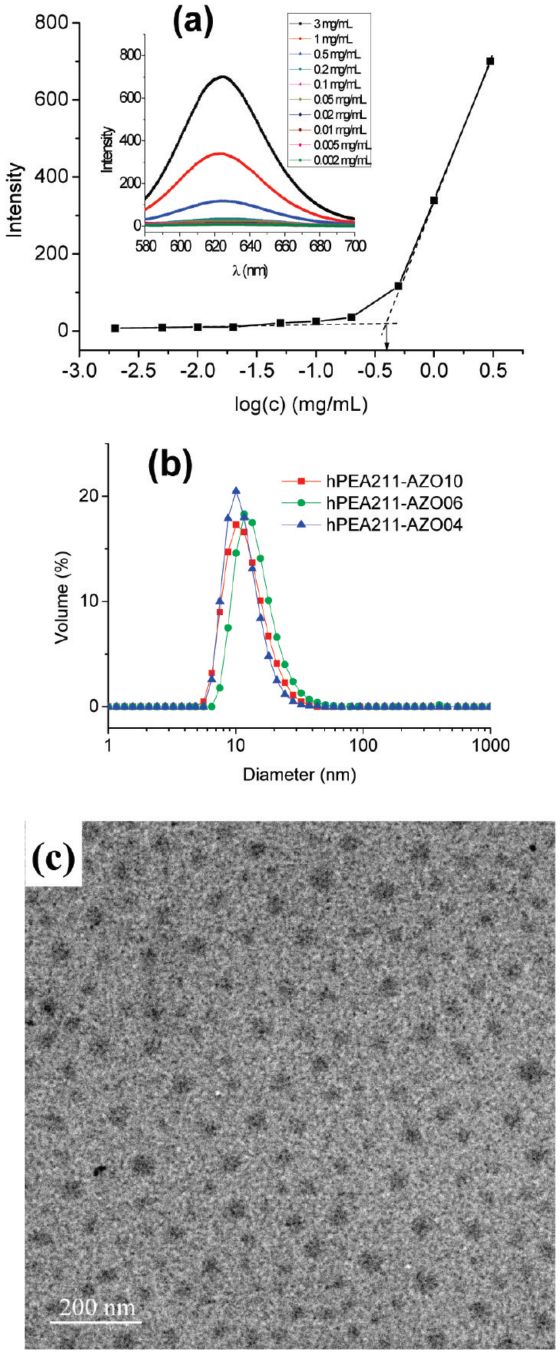

Figure 2. (a) Plot of the maximum fluorescence emission intensity of the Nile Red vs concentration of hPEA211-AZO06. Inset: fluorescence emission spectra of Nile Red solution with different hPEA211-AZO06 concentration. (b) Size distribution of nanoparticles formed by hPEA211-AZO10, hPEA211-AZO06, and hPEA211-AZO04 determined by DLS at 25 °C in aqueous solution. Polymer concentration is 1 mg/mL. (c) TEM image of the nanoparticles formed by hPEA211-AZO10 at room temperature.

Table 2. Characterization of hPEA211-AZO Nanoparticles

	cloud point (°C)[a]			average diameter (nm)[b]	
nanoparticles	CP_T	CP_C	ΔCP	trans	cis
hPEA211-AZO02	72.4	71.7	0.7	10.4 ± 1.5	12.5 ± 3.3
hPEA211-AZO04	60.3	58.5	1.8	11.9 ± 1.6	16.5 ± 1.7
hPEA211-AZO06	49.6	46.8	2.8	15.0 ± 2.7	18.8 ± 0.8
hPEA211-AZO08	41.8	37.8	4.0	18.3 ± 3.3	21.2 ± 2.3
hPEA211-AZO10	30.2	24.9	5.3	12.5 ± 1.9	16.3 ± 2.2

[a] Cloud point was determined by a UV−visible spectrophotometer equipped with a thermo cell. All the samples were prepared at pH 7.4 with 3 mg/mL polymer concentration. CP_T was tested as soon as the samples were prepared, while CP_C was tested after UV irradiation (365 nm) for 40 min. ΔCP is calculated as $CP_T - CP_C$ [b] The average diameters of the nanoparticles based on hPEA211-AZO were determined by DLS spectra. All the samples were prepared using ultrapure water with 1 mg/mL polymer concentration and tested at 25 °C. The diameter with azobenzene moieties in *trans* form was tested as soon as the samples were prepared while the diameter with azobenzene moieties in *cis* form was tested after UV irradiation (365 nm) for 40 min. The error range was calculated as the standard deviation of five times of measurement.

indicating that the proportion of amino groups of hPEA211 modified by azobenzene is tunable by the amount of E-AZO in feed during the synthesis process.

Formation and Morphology of the hPEA211-AZO Nanoparticles. Just as amphiphilic hPEA211, hPEA211-AZOs were expected to self-assemble directly into nanoparticles in water, which are comprised of hydrophobic PPO chains and azobenzene moieties as core and hydrophilic PEO chains as shell. As a strong evidence for self-assembly behavior of amphiphilic polymer into nanoparticles, critical micelle concentration (CMC) value for hPEA211-AZO was determined by a fluorescence spectroscopy using Nile Red as a fluorescence probe.[38] Figure 2a shows the maximum fluorescence intensity as a function of the logarithm of hPEA211-AZO06 concentration ranging from 0.002 g/L to 3 g/L, from which a sudden increase of the maximum fluorescence intensity is observed at the concentration of about 0.38 g/L, indicating the formation of the micelles. The CMCs of other hPEA211-AZO at room temperature are measured by the same method, and the results are summarized in Table 1.

The formation of nanoparticles from hPEA211-AZOs was further investigated by dynamic light scattering (DLS) experiments, a series of 1 mg/mL hPEA211-AZO aqueous solutions were measured at 25 °C. The polymer concentration is higher than CMC to ensure the formation of nanoparticles. Taking hPEA211-AZO10 as example, the size distribution of hPEA211-AZO10 nanoparticle is shown in Figure 2b, which indicated the formation of uniform-sized nanoparticle with diameter of about 12.53 ± 1.90 nm and polydispersity index (PDI) of 0.327. The size of all hPEA211-AZO nanoparticles determined by DLS is summarized in Table 2. The morphology of hPEA211-AZO10 nanoparticles was revealed by TEM (Figure 2c). It should be noted that the diameter of the nanoparticles determined by TEM is bigger than that of DLS analysis. This might be ascribed that the nanoparticles were somewhat flattened on the copper grids in TEM experiments.[39−42]

The Behavior of hPEA211-AZO Nanoparticles Responsive to Temperature, pH, and Ionic Strength. hPEA211-AZO nanoparticles were designed to be responsive to temperature, pH, and ionic strength. hPEA211-AZO nanoparticles are comprised of hydrophobic azobenzene moieties and PPO short chains as core and hydrophilic PEO short chains as outer shell, which prevents the nanoparticles from aggregating further. With the increase of temperature, hydrogen bonds between water molecules and hydrophilic part of the nanoparticles are destroyed. The outer shell becomes less hydrophilic, leading to the aggregation of hPEA211-AZO nanoparticles and the turbidity of the solutions. The thermal responsive aggregation behaviors of hPEA211-AZO nanoparticles under different conditions were investigated by measuring their cloud point (CP). As can be seen in Figure 3a, the transmittances of all hPEA211-AZO aqueous solution exhibit a sharp decrease above their CPs. With the increase of the proportion of amino groups in hPEA211 modified by azobenzene from 0.2 to 1.0, CP decreases from 72.4 to 30.2 °C, indicating that the proportion of amino groups modified by azobenzene has obvious effect on CP. Because of the higher hydrophobicity of azobenzene moieties in comparison with terminal amino groups, increasing of the azobenzene proportion can make hPEA211-AZO more

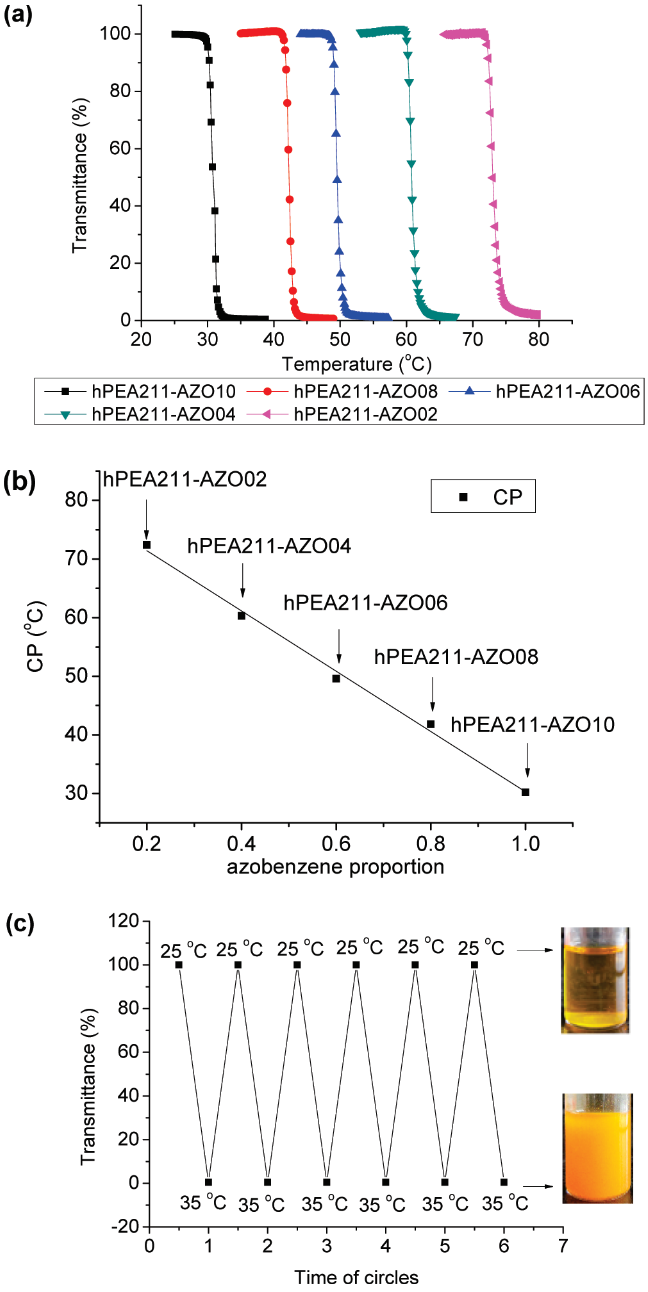

Figure 3. (a) Temperature dependence of optical transmittance at 700 nm for hPEA211-AZO aqueous solution at pH 7.4. (b) CP of 3 mg/mL hPEA211-AZO aqueous solutions at pH 7.4 as a function of the proportion of amino groups in hPEA211 modified by azobenzene. (c) Reversible change of transmittance at 700 nm for hPEA211-AZO10 aqueous solution at pH 7.4 between 25 and 35 °C.

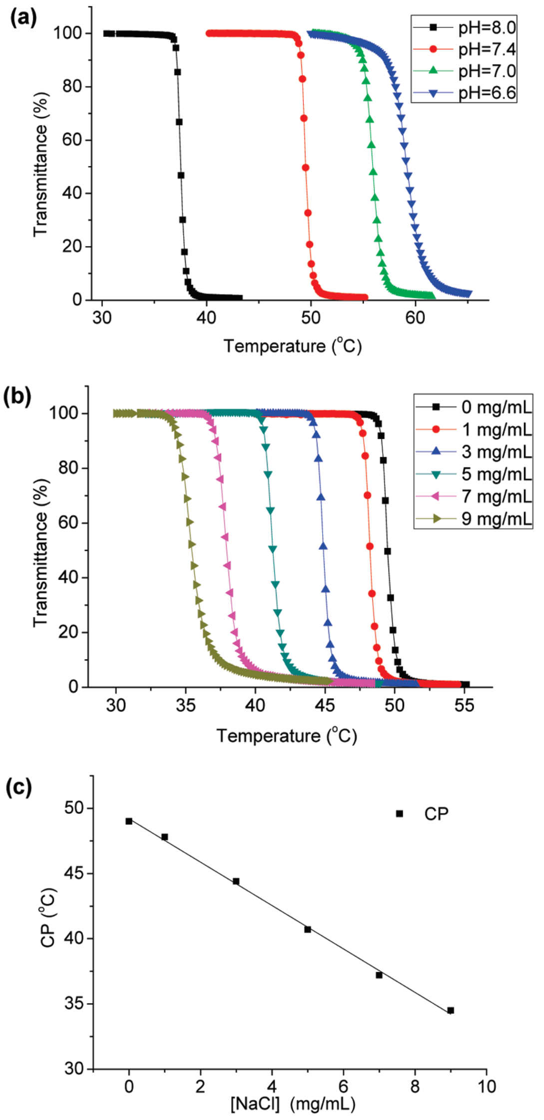

Figure 4. (a) pH dependence of optical transmittance at 700 nm for hPEA211-AZO06 aqueous solution. (b) NaCl concentration dependence of optical transmittance at 700 nm for hPEA211-AZO06 aqueous solution at pH 7.4. (c) the effect of NaCl concentration on the CP of 3 mg/mL hPEA211-AZO06 aqueous solution at pH 7.4.

hydrophobic, resulting in a lower CP. Figure 3b shows the relationship between CP and azobenzene proportion at pH 7.4. A good linear relationship ($y = 81.61 - 51.4x$) was obtained between the CP and azobenzene proportion, suggesting well-tunable CP of hPEA211-AZO aqueous solution. It should be noted that the thermal-responsive behavior of hPEA211-AZO nanoparticles is completely reversible, which can be confirmed by Figure 3c. After several circles of heating to cooling, hPEA211-AZO aqueous solution is still transparent.

Because amino groups in the backbone and periphery of hPEA211-AZO can be protonated and deprotonated at different pH, hPEA211-AZO aqueous solution also exhibits a response to pH. Figure 4a shows a typical transmittance versus temperature at different pH for hPEA211-AZO06 aqueous solution, which indicates that CP of hPEA211-AZO06 decrease from 57.2 to 37.1 °C with increasing of pH value from 6.6 to 8.0. This can be explained by the fact that deprotonation of amino groups at a higher pH reduces the hydrophilicity of the outer shell of nanoparticles, resulting in aggregation at a lower temperature.

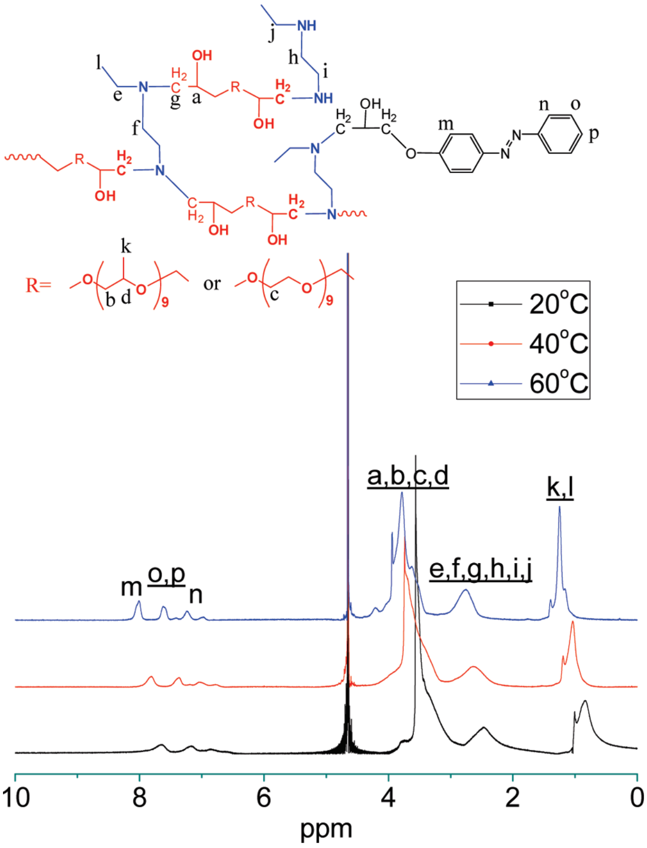

Figure 5. ^{1}H NMR spectra of 1 wt % hPEA211-AZO06 in D_2O at different temperatures.

Because salt has influence on the hydrogen bond between PEO chains and water molecules, hPEA211-AZO nanoparticles in aqueous solution are also expected to be responsive to ionic strength. Figure 4b shows transmittance versus temperature for hPEA211-AZO06 at different NaCl concentrations, which indicates that CP decreases with the increase of NaCl concentration. Figure 4c shows CP recorded for hPEA211-AZO06 in the presence of increasing amount of NaCl. CP decreases very obviously from 49.0 to 34.5 °C with the increase of NaCl concentration from 0 to 9 mg/mL, indicating that hPEA211-AZO nanoparticles are very sensitive to ionic strength. It is interesting that a linear relationship ($y = 49.2 - 1.66x$) can be obtained between the CP and NaCl concentration. These results can be explained by salt-out effect.[43,44] The presence of NaCl might lead to partial dehydration of PEO chains, resulting in a decrease of the CP.

The responsive aggregation behavior of hPEA211-AZO nanoparticles in aqueous solution is further investigated by ^{1}H NMR spectra (Figure 5). As PPO chains are not hydrophobic completely, the signals of methyl can be observed at 20 °C, while azobenzene moieties are more hydrophobic, and the signals of azobenzene cannot be obviously observed at 20 °C. With the increase of the temperature above CP, PPO segments become more hydrophobic and some of which associate together to form hydrophobic cores; at the same time, the hydrophilic shell layer formed by PEO chains are dehydrated and shrink. The compression of PEO shell at high temperature might cause that part of hydrophobic core appear outside. As a result, the signals of azobenzene can be also obviously observed at 60 °C, which is similar to coumarin-contained linear poly(ether amine) in our previous study.[45] A possible process for responsive aggregation of hPEA211-AZO in water is proposed in Scheme 2. hPEA211-AZOs are dispersed directly as nanoparticles in aqueous solution, which are composed of PPO chains and azobenzene moieties as hydrophobic cores while PEO chains and amino moieties as hydrophilic shells. With increase of the temperature, the hydrogen bonds between PEO chains and water are destroyed, which decreased the hydrophilicity of PEO shell, resulting in aggregation of these nanoparticles into large particles.

The Behavior of hPEA211-AZO Nanoparticles Responsive to Light. As hPEA211-AZO nanoparticles are comprised of photoswitchable azobenzene as cores, the light-responsive behavior was investigated. We traced the isomerization of azobenzene under irradiation of 365 and 450 nm wavelength by UV−vis spectra (Figure 6). There are two major absorption bands, one is at ∼343 nm attributed to the $\pi-\pi^*$ transition of the azobenzene, the other is at ∼435 nm attributed to the $n-\pi^*$ transition. Under the irradiation of 365 nm, $\pi-\pi^*$ transition adsorption of azobenzene at 343 nm decreased with the increase of irradiation time, while $n-\pi^*$ transition at 435 nm increased, suggesting the isomerization of azobenzene from *trans* to *cis* form (Figure 6a). It should be noted that the process of isomerization from *trans* to *cis* form lasts for about 40 min, which is much slower than some other azobenzene-contained polymer reported.[17,25−27] Then the hPEA211-AZO10 aqueous solution after UV irradiation is exposed under visible light of 450 nm, and the changes of UV−vis spectra are shown in Figure 6b, the process of back-conversion from *cis* to *trans* form only lasts for 10 min,[25,27] which is more rapid than the isomerization from *trans* to *cis* form. This might be ascribed to the close packing of azobenzene in the core of nanoparticles. Because the *trans* form of azobenzene is easier to pack closely than the *cis* form, the isomerization from *trans* to *cis* form in the core of nanoparticles is limited, which consequently lead to the slow conversion. This can be further verified by the following DLS and AFM experiments, and will be discussed later.

Because the isomerization of azobenzene is accompanied by the change of dipole moment of the molecular structure, the CP of nanoparticles comprised of azobenzene core is expected to be shifted upon irradiation of UV-light. We measured the CP of hPEA211-AZO nanoparticles in aqueous solution again after irradiation of UV-light (365 nm) for 40 min. As an example, the temperature dependence of optical transmittance for hPEA211-AZO08 and hPEA211-AZO06 aqueous solution before and after UV irradiation is illustrated in Figure 7. It is really surprised that lower CPs for all hPEA211-AZO aqueous solutions were observed after UV irradiation (365 nm), and the differences of CP between nonirradiated (*trans*) and irradiated (*cis*) hPEA211-AZO nanoparticles in aqueous solution increased linearly upon the azobenzene content up to 5.3 °C (Table 2 and Figure S2 (Supporting Information)). For most of the responsive polymers containing azobenzene reported,[23,26] however, the lowest critical soluble temperature (LCST) became higher

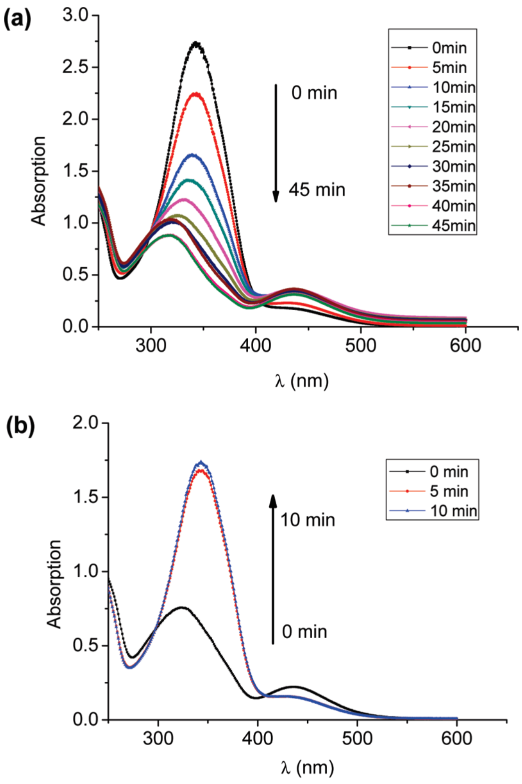

Figure 6. (a) Dependence of UV−vis spectra of hPEA-AZO10 aqueous solution at pH 7.4 on UV irradiation (365 nm) time. (b) Dependence of UV−vis spectra of hPEA-AZO10 aqueous solution at pH 7.4 on visible light irradiation (450 nm) time. Polymer concentration is 3 mg/mL, diluted into 0.1 mg/mL when it is tested.

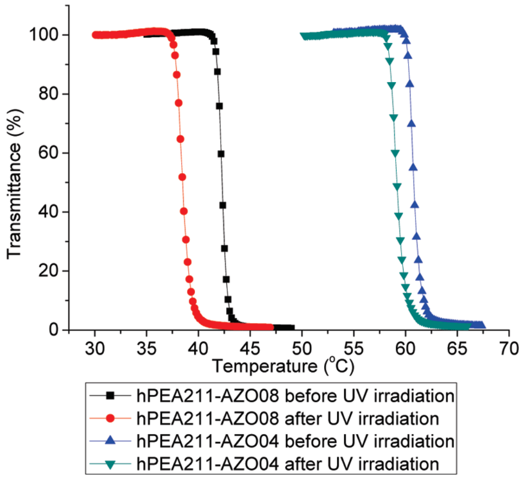

Figure 7. Temperature dependence of optical transmittance at 700 nm for hPEA211-AZO aqueous solution at pH 7.4 before and after UV irradiation (365 nm) for 40 min,.

Scheme 2. Proposed Mechanism for Phase Transition of hPEA211-AZO Aqueous Solution

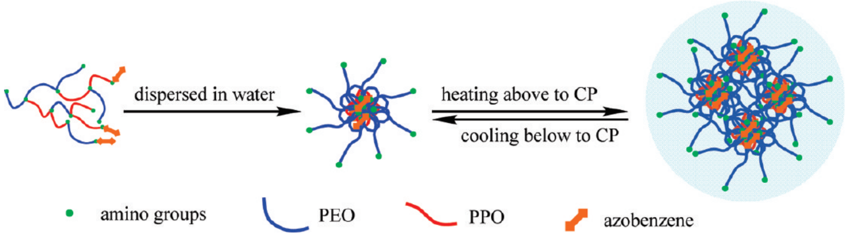

after irradiation of 365 nm light, which was explained by an increase in dipole moment of the *cis* form and thus an increased local polarity of the polymer chain. The reason why CP decreases after irradiation of 365 nm light might be attributed that hPEA211-AZOs are dispersed as nanoparticles instead of single polymer chain in water.

To understand what happened to hPEA211-AZO nanoparticles after UV irradiation (365 nm), DLS experiments were conducted. The size distribution of hPEA211-AZO10 aqueous solution before and after UV irradiation is shown in Figure 8, which indicates that the average diameter of the hPEA211-AZO10 nanoparticles increases from 12.5 ± 1.9 nm to 16.3 ± 2.2 nm after UV irradiation. Similar results are also obtained by DLS measurements of the other hPEA211-AZO nanoparticles, which are summarized in Table 2. The increase of the size of hPEA211-AZO nanoparticles is further confirmed by the AFM images of hPEA211-AZO10 in aqueous solution. As shown in Figure 9, the size of hPEA211-AZO10 nanoparticles increases from ~25 nm to ~35 nm after UV irradiation of 365 nm. The diameter determined by AFM is larger than that of DLS analysis, which might be resulted from that the nanoparticles were somewhat flattened on the mica sheet in AFM experiments,

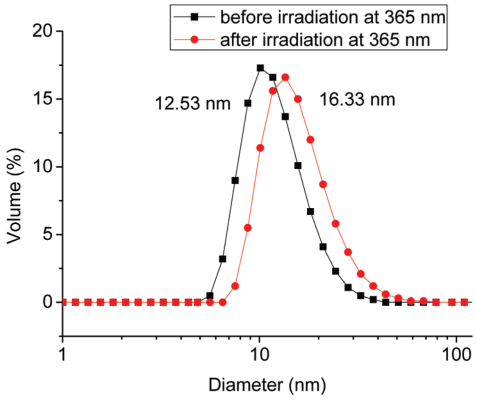

Figure 8. Size distribution of hPEA211-AZO10 aqueous solution at pH 7.4/25 °C before and after UV irradiation (365 nm) for 40 min.

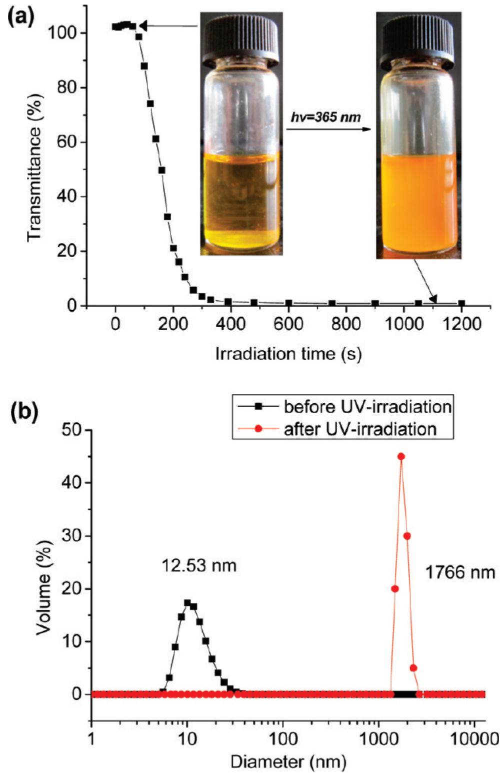

Figure 10. (a) Dependence of optical transmittance at 700 nm for hPEA211-AZO10 aqueous solution on irradiation time at 365 nm at pH 7.4/28 °C and photograph before and after phase transition. Polymer concentration is 3 mg/mL. (b) Size distribution of hPEA211-AZO10 aqueous solution at pH 7.4/25 °C before and after UV irradiation (365 nm) for 40 min.

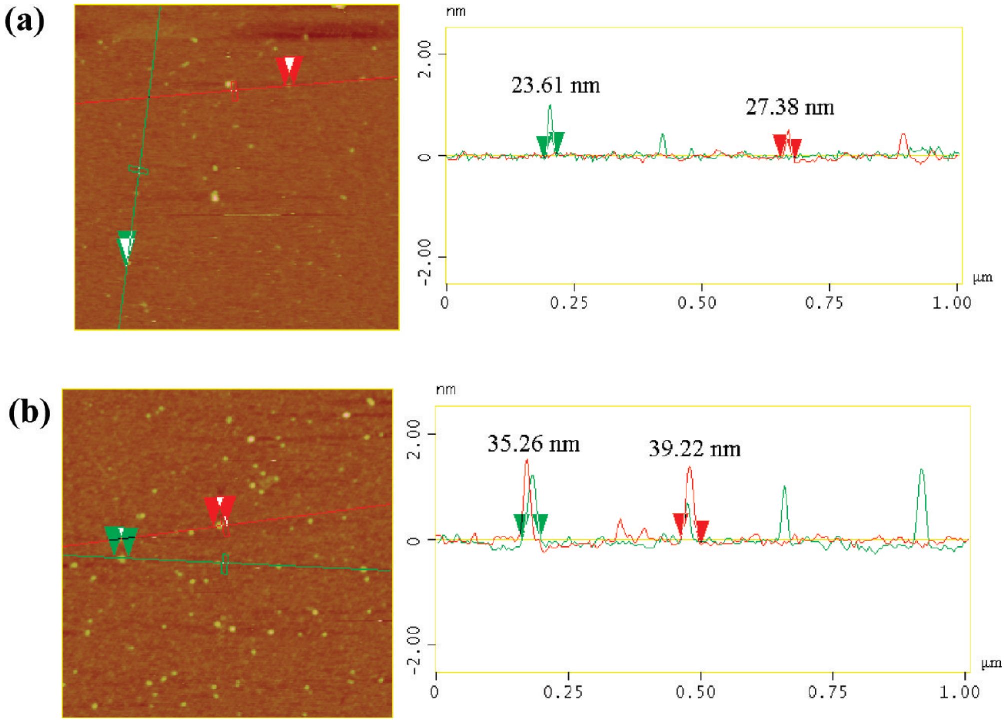

Figure 9. AFM images of hPEA211-AZO10 in aqueous solution: (a) before UV irradiation; (b) after UV irradiation (365 nm) for 40 min.

Scheme 3. Proposed Mechanism of the Light Response of hPEA211-AZO Aqueous Solution

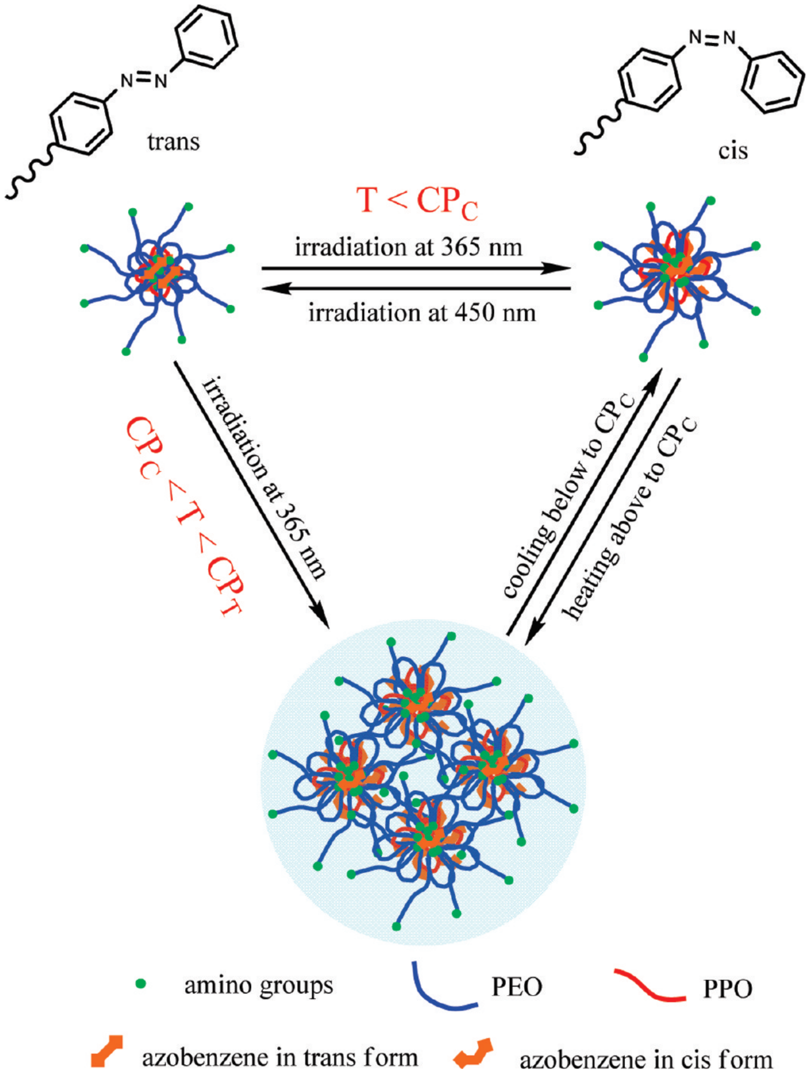

and this phenomenon is also proved by the height profiles of the AFM images in Figure 9. The increase of the size of hPEA211-AZO10 nanoparticles after UV irradiation should be caused by the isomerization of azobenzene from *trans* to *cis* form. Because the *trans* form of azobenzene is more regular, the *cis* form can not pack as closely as *trans* form in the core of hPEA211-AZO10 nanoparticles, resulting in the increase of the size of the core. Because of the looser packing of the *cis* form in the core, the isomerization from *cis* to *trans* form should be faster under visible light irradiation (450 nm) than that from *trans* to *cis* form, which explains the results from Figure 6.

Taking the structure of hPEA211-AZO nanoparticles into consideration, the polarity of azobenzene has little effect on CP of hPEA211-AZO nanoparticles as most of the azobenzene moieties are in the core, which have no interact with water molecules. At the same time, the nanoparticles are stabilized by the hydrophilic PEO shell which prevents them from aggregating together in aqueous solution. During UV irradiation, the size of hPEA211-AZO nanoparticles becomes larger slowly. When the core of the nanoparticles becomes large enough and the hydrophilic PEO shell may not be sufficient to stabilize the nanoparticles, these nanomicelles will aggregate at lower temperature. Therefore, the larger size of hPEA211-AZO nanoparticles induced by UV irradiation (365 nm) is believed to be the key factor to cause the CP shift to the lower temperature.

Accordingly, light-induced aggregation of hPEA211-AZO nanoparticles was possible within the temperature range between CP_C (*cis* form, after UV irradiation) and CP_T (*trans* form, before irradiation). Taking hPEA211-AZO10 as an example, Figure 10a illustrated the dependence of optical transmittance for hPEA211-AZO10 aqueous solution on UV irradiation time with inset of the photographs. hPEA211-AZO10 can be dispersed in water at 28 °C to form an orange transparent aqueous solution, and its optical transmittance at 700 nm is about 100%. After UV irradiation, the optical transmittance of the hPEA211-AZO10 aqueous solution decreases sharply to ~0% at about 400 s, and the solution turns into orange opaque suspension. This phenomenon can also be supported by DLS experiments, and the results are shown in Figure 10b. After UV irradiation, only one peak with an average diameter ~1800 nm was observed in DLS experiment, suggesting the light-induced aggregation of the nanoparticles. As a result, the hPEA211-AZO10 aqueous solution turned opaque. On the basis of these results, the proposed mechanism for the light-induced change of the morphology of hPEA211-AZO nanoparticles in aqueous solution was illustrated in Scheme 3. UV irradiation (365 nm) can make hPEA211-AZO nanoparticles become larger nanoparticles or aggregate into microparticles, which is dependent on the temperature range.

Conclusion

A series of hPEA211-AZOs were synthesized by introduction of azobenzene moieties into the periphery of hyperbranched poly(ether amine) (hPEA211). The obtained hPEA211-AZOs can self-assemble directly into nanoparticles with diameter of 10−18 nm in aqueous solution, which exhibited very sharp response to temperature, pH, ionic strength and light with well-tunable CP from 25 to 90 °C. After UV irradiation (365 nm), the lower value of CP was observed, which is believed to be caused by the larger size of hPEA211-AZO nanoparticles. The CP difference of hPEA211-AZO nanoparticles in aqueous solution between before (*trans* form) and after (*cis* form) UV irradiation increases linearly upon the azobenzene content up to 5 °C.

Acknowledgment. We thank the National Nature Science Foundation of China (No: 50803036) and Science & Technology Commission of Shanghai Municipal Government (No: 08520704700) for their financial support.

Supporting Information Available: Figures showing FT-IR spectra of hPEA211, E-AZO, and hPEA211-AZO10 and a plot of CP and ΔCP of 3 mg/mL hPEA211-AZO aqueous solutions at pH 7.4 during irradiation as a function of azobenzene content in hPEA211-AZO. This material is available free of charge via the Internet at http://pubs.acs.org.

References and Notes

(1) Owens, D. E.; Jian, Y. C.; Fang, J. E.; Slaughter, B. V.; Chen, Y. H.; Peppas, N. A. *Macromolecules* **2007**, *40*, 7306–7310.
(2) Zhang, Y. F.; Luo, S. Z.; Liu, S. Y. *Macromolecules* **2005**, *38*, 9813–9820.
(3) Hantzschel, N.; Zhang, F. B.; Eckert, F.; Pich, A.; Winnik, M. A. *Langmuir* **2007**, *23*, 10793–10800.
(4) O'Reilly, R. K.; Hawker, C. J.; Wooley, K. L. *Chem. Soc. Rev.* **2006**, *35*, 1068–1083.
(5) Vancaeyzeele, C.; Ornatsky, O.; Baranov, V.; Shen, L.; Abdelrahman, A.; Winnik, M. A. *J. Am. Chem. Soc.* **2007**, *129*, 13653–13660.
(6) Klaikherd, A.; Nagamani, C.; Thayumanavan, S. *J. Am. Chem. Soc.* **2009**, *131*, 4830–4838.
(7) Bromberg, L. E.; Ron, E. S. *Adv. Drug Deliv. Rev.* **1998**, *31*, 197–221.
(8) Willet, N.; Gohy, J. F.; Auvray, L.; Varshney, S.; Jerome, R.; Leyh, B. *Langmuir* **2008**, *24*, 3009–3015.
(9) Kikuchi, A.; Okano, T. *Prog. Polym. Sci.* **2002**, *27*, 1165–1193.
(10) VandenMooter, G.; Maris, B.; Samyn, C.; Augustijns, P.; Kinget, R. *J. Pharm. Sci.* **1997**, *86*, 1321–1327.
(11) Mahkam, M.; Assam, M. G.; Zahedifar, R.; Ramesh, M.; Davaran, S. *J. Bioact. Compat. Polym.* **2004**, *19*, 45–53.
(12) Lai, J. Y.; Tu, K. H.; Wang, H. J.; Chen, Z. G.; Wang, L. Q. *J. Appl. Polym. Sci.* **2008**, *108*, 3305–3312.
(13) Loudwig, S.; Bayley, H. *J. Am. Chem. Soc.* **2006**, *128*, 12404–12405.
(14) Inoue, Y.; Kuad, P.; Okumura, Y.; Takashima, Y.; Yamaguchi, H.; Harada, A. *J. Am. Chem. Soc.* **2007**, *129*, 6396–6397.
(15) Ferri, V.; Elbing, M.; Pace, G.; Dickey, M. D.; Zharnikov, M.; Samori, P.; Mayor, M.; Rampi, M. A. *Angew. Chem., Int. Ed.* **2008**, *47*, 3407–3409.
(16) Li, Y. B.; Deng, Y. H.; He, Y. N.; Tong, X. L.; Wang, X. G. *Langmuir* **2005**, *21*, 6567–6571.
(17) Li, Y. B.; Deng, Y. H.; Tong, X. L.; Wang, X. G. *Macromolecules* **2006**, *39*, 1108–1115.
(18) Ma, N.; Wang, Y. P.; Wang, B. Y.; Wang, Z. Q.; Zhang, X.; Wang, G.; Zhao, Y. *Langmuir* **2007**, *23*, 2874–2878.
(19) Lin, S. L.; Numasawa, N.; Nose, T.; Lin, J. P. *Macromolecules* **2007**, *40*, 1684–1692.
(20) Akiyama, H.; Tamaoki, N. *Macromolecules* **2007**, *40*, 5129–5132.
(21) Jochum, F. D.; zur Borg, L.; Roth, P. J.; Theato, P. *Macromolecules* **2009**, *42*, 7854–7862.
(22) Wang, G.; Tong, X.; Zhao, Y. *Macromolecules* **2004**, *37*, 8911–8917.
(23) Tong, X.; Wang, G.; Soldera, A.; Zhao, Y. *J. Phys. Chem. B* **2005**, *109*, 20281–20287.
(24) Qi, B.; Zhao, Y. *Langmuir* **2007**, *23*, 5746–5751.
(25) Deshmukh, S.; Bromberg, L.; Smith, K. A.; Hatton, T. A. *Langmuir* **2009**, *25*, 3459–3466.
(26) Alonso, M.; Reboto, V.; Guiscardo, L.; Mate, V.; Rodriguez-Cabello, J. C. *Macromolecules* **2001**, *34*, 8072–8077.
(27) Zhao, Y.; Tremblay, L.; Zhao, Y. *J. Polym. Sci., Polym. Chem.* **2010**, *48*, 4055–4066.
(28) Goodwin, A. P.; Mynar, J. L.; Ma, Y. Z.; Fleming, G. R.; Frechet, J. M. J. *J. Am. Chem. Soc.* **2005**, *127*, 9952–9953.
(29) Morishima, Y. *Angew. Chem., Int. Ed.* **2007**, *46*, 1370–1372.
(30) Zhang, Q.; Clark, C. G.; Wang, M.; Remsen, E. E.; Wooley, K. L. *Nano Lett.* **2002**, *2*, 1051–1054.
(31) Jung, J.; Lee, I. H.; Lee, E.; Park, J.; Jon, S. *Biomacromolecules* **2007**, *8*, 3401–3407.
(32) Apostolovic, B.; Klok, H. A. *Biomacromolecules* **2008**, *9*, 3173–3180.
(33) Li, C. M.; Madsen, J.; Armes, S. P.; Lewis, A. L. *Angew. Chem., Int. Ed.* **2006**, *45*, 3510–3513.
(34) Mano, J. F. *Adv. Eng. Mater.* **2008**, *10*, 515–527.
(35) Li, J. L.; Bai, R. B.; Chen, B. H. *Langmuir* **2004**, *20*, 6068–6070.
(36) Rapoport, N. *Prog. Polym. Sci.* **2007**, *32*, 962–990.
(37) Yu, B.; Jiang, X. S.; Yin, G. L.; Yin, J. *J. Polym. Sci., Polym. Chem.* **2010**, *48*, 4252–4261.
(38) Trimaille, T.; Mondon, K.; Gurny, R.; Moller, M. *Int. J. Pharm.* **2006**, *319*, 147–154.
(39) Hua, C.; Dong, C. M. *J. Biomed. Mater., Res. A* **2007**, *82A*, 689–700.
(40) Liu, L.; Guo, S. R.; Chang, J.; Ning, C. Q.; Dong, C. M.; Yan, D. Y. *J. Biomed. Mater., Res. B* **2008**, *87B*, 244–250.
(41) Narain, R.; Armes, S. P. *Biomacromolecules* **2003**, *4*, 1746–1758.
(42) Liu, S. Y.; Armes, S. P. *Angew. Chem., Int. Ed.* **2002**, *41*, 1413–1416.
(43) Alexandridis, P.; Holzwarth, J. F. *Langmuir* **1997**, *13*, 6074–6082.
(44) Lutz, J. F.; Akdemir, O.; Hoth, A. *J. Am. Chem. Soc.* **2006**, *128*, 13046–13047.
(45) Jiang, X. S.; Wang, R.; Ren, Y. R.; Yin, J. *Langmuir* **2009**, *25*, 19629–9632.